OIL BLENDING: MIXING AND CONTAMINATION

The Shell Company of Australia has a frequent need to blend lubricants. Blending, sometimes involving three lubricant oils and additives, takes place by jet mixing in large tanks of typically 45,000 litres capacity. The jets are driven by pumps with typical volume throughput of up to 1,000 litres per minute, and typical blending times may be as long as one or two hours.

The jet blending process was investigated in a number of ways at the Study Group. These included: simple estimates for blending times, theoretical and experimental description of jet behaviour, development of a simple compartment model for the blending process, and several large scale computer simulations of the jet-induced motion using a commercial Computational Fluid Dynamics package. In addition, the sedimentation of contaminant particles in the tanks was investigated. This overall investigation, using a variety of approaches, gave a good knowledge of the blending process.

1. Introduction

The topic was introduced by Mr Colin Macpherson, Production Services Manager for Shell Australia. Figure 1 contains a schematic of the oil blending process. The mixing tank can be as large as a domestic swimming pool, typically 45,000 litres in capacity, whilst the jet mixing is driven by a pump of typically 1,000 litres per minute capacity. Additives are usually mixed in with the various oils before they are poured into the tank. Typically, the oils are similar in density but quite different in viscosity. The oils usually have similar molecular structure, are miscible in each other, and stay mixed once they have been mixed by the jet blending process. The viscosity of the oils is strongly temperature dependent and some heating of the mixing tank is often used to assist the blending process, particularly in cold climates.

The lubricant mixture invariably contains many small contaminant particles whose overall concentration is controlled by International Standards No. 4406. The contaminant particles are silicates, small metal particles, and small wax particles that eventually are soluble in the lubricant mix.

The main objectives of the investigation were

- to understand the jet blending process
- to gain good estimates of the time required to mix the lubricants
- to suggest ways in which the process could be optimised, for example through placement and design of the nozzle

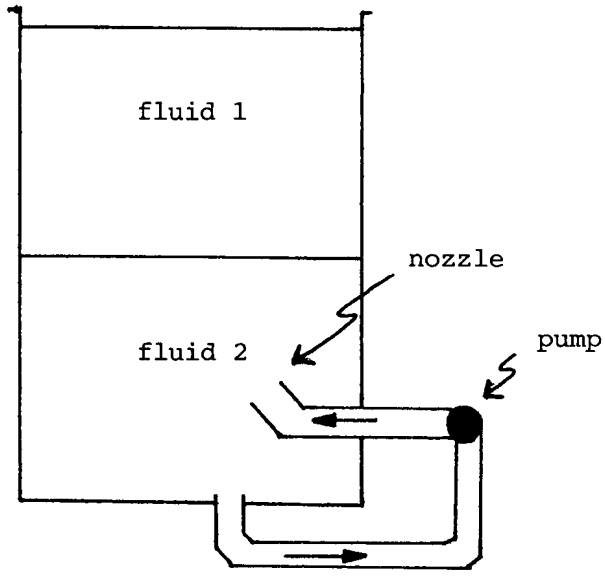

Figure 1: Illustrating the oil blending process.

- to understand the sedimentation of particles in a well-mixed blend

These objectives were addressed in various ways at the Study Group. In particular, Section 2 contains simple estimates of the time required to blend the lubricants, assuming the blending process is highly efficient. In Section 3, we review the theoretical and experimental literature on turbulent jets, and point out that the near jet behaviour is largely independent of the physical properties of the fluid through which it passes. Section 4 contains an idealised compartment model and numerical simulation of the mixing process. For theoretical and numerical tractability, this model is necessarily axi-symmetric, but we believe it incorporates many of the actual features of the process. For the purposes of simplifying initial conditions, a two layered initial state has been used. In Section 5, the commercial Computational Fluid Dynamics (CFD) code *FIDAP* is used to compute the mean flow field caused by one particular placement of the submerged jet near the bottom of the tank. The sedimentation aspects are examined in Section 6: these proved to be surprisingly simple to investigate since the contaminant particles are both extremely small and widely separated. Results are presented graphically to show the sedimentation time of various particles and hence the storage lifetime of oil blends.

Lastly, Section 7 summarises the outcomes of work on this problem at the Study Group and points out the main features that remain incomplete. To highlight the results, substantial progress has been made on the various goals listed above, and the framework for detailed CFD investigations has been established should there be a need for investigation of details of design.

2. Features of significance, simple estimates for mixing times

A detailed model for the oil blending problem has many features that need to addressed, such as

- layers of oils with different viscosities, initially with an interface between the layers
- heating and temperature dependent viscosities
- turbulence induced by the oil jet driven by the pump
- the fine details of the mixing process
- the free surface at the top of the oil tank
- the complex three dimensional geometry of the mixing tanks

The Reynolds number of the oil jet driven by the pump is of great importance. If the jet has nozzle diameter d and emits a volume flux F, then the mean speed of the nozzle is $\bar{V} = 4F/\pi d^2$. The typical values $F = 1{,}000$ lit/min $= 1/60$ m^{3}s^{-1} and $d = 0.03$ m then give $\bar{V} \approx 24$ ms^{-1}. The Reynolds number of the jet is $Re = \bar{V}d/\nu$ where ν is the kinematic viscosity of the oil, for which a representative value is 2×10^{-5} m^{2}s^{-1}. This gives the nozzle Reynolds number $Re \approx 3.6 \times 10^4$.

The jet is certainly turbulent at these Reynolds numbers, although it does not follow that all of the mixing tank exhibits turbulence. Indeed, consider mixing in a cylindrical tank of internal diameter 2.2 m. Without considering entrainment into the jet, suppose that 1,000 litres of oil per minute move upwards in the jet whilst, in the remainder of the tank, 1,000 litres per minute move downwards. Suppose that the jet at a certain level is confined to one quarter of the tank's cross-section. Then the mean downwards speed is approximately 0.00146 ms^{-1}, and the Reynolds number for the bulk of the tank is $Re_{tank} \approx 0.00146 \times 2.2/2 \times 10^{-5} \approx 160$, for which laminar flow is expected. Hence we have the picture of a turbulent jet in an almost quiescent fluid. Further details of the jet and its entrainment of fluid are given in the next Section.

The oil jet is an indirect mechanism for blending the oil, and any individual sample of oil has surprisingly little chance of being cycled through the pump. Suppose the tank

is perfectly mixed, and we consider a small sample in a 45,000 litre tank with 1,000 litre/min pump. In one minute, the sample has a probability of 44/45 of avoiding the pump. More generally the probability of avoiding the pump is

mins	0	1	30	60	120	180	240
% chance	100	97.8	51.0	26.0	6.7	1.75	0.45

Note that 0.45% of 45,000 litres is 205 litres. Clearly the mixing of oil takes place indirectly, and not by passage through the pump.

A second simple estimate can be made for the mixing time of a 100 ml sample of oil. Divide the 45,000 litre tank into N equal layers, $L_1, ..., L_N$, each of which is perfectly mixed; 1,000 litres moves upwards and 1,000 litres downwards in each minute. Let A_i denote the amount of the sample in layer i. After one minute's mixing, A_i will change by

$$(A_{i-1} - 2A_i + A_{i+1})\frac{1000}{45000/N}$$

This leads to the results in Tables 1 and 2.

Table 1. Mixing of 100 ml through 9 layers, oil originally in L_1

mins	L_1	L_2	L_3	L_4	L_5	L_6	L_7	L_8	L_9
0	100.0	0.0	0.0	0.0	0.0	0.0	0.0	0.0	0.0
30	20.4	18.8	16.2	13.3	10.3	7.6	5.6	4.2	3.6
60	14.7	14.1	13.2	12.1	11.0	9.8	8.9	8.2	8.0
120	11.7	11.6	11.5	11.3	11.1	10.9	10.8	10.7	10.6

Table 2. Mixing of 100 ml oil through 9 layers, oil originally in L_5

mins	L_1	L_2	L_3	L_4	L_5	L_6	L_7	L_8	L_9
0	0.0	0.0	0.0	0.0	100.0	0.0	0.0	0.0	0.0
30	10.8	11.1	11.5	11.8	11.8	11.4	10.9	10.5	10.3
90	11.2	11.2	11.2	11.1	11.1	11.1	11.1	11.1	11.1

The results show that a 100 ml sample of oil will diffuse reasonably thoroughly throughout a 45,000 litre tank in about an hour provided that some 1,000 litres per minute are exchanged between adjacent layers. The results in Table 2 should be symmetric about L_5; the minor asymmetry occurs because of the implementation of the above algorithm.

3. Review of properties of turbulent jets

From Section 2, we recall the image of a turbulent jet with Reynolds number greater than 30,000 discharging into an almost quiescent bath of oil. The properties of such jets are very well known, see for example Fischer *et al.* (1979, chapter 9). In brief, the jet entrains oil from the surrounding fluid, thereby increasing the radius of the jet and increasing the volume flux, whilst maintaining the Reynolds number and momentum of the jet at constant values. The speed of the jet decreases with axial distance.

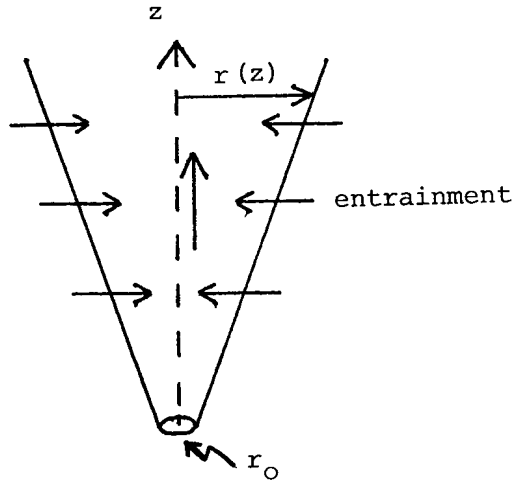

Figure 2: Definition sketch for the turbulent jet.

These concepts can be expressed simply in mathematical terms. Suppose the distance along the axis of the jet is z, the radius of the jet is $r(z)$, the mean speed of the jet is u and the volume flux of the jet is Q. A subscript zero indicates values at the nozzle.

Conservation of momentum in the jet requires that

$$u_0 Q_0 = uQ \tag{1}$$

and by definition we have

$$Q = \pi r^2 u \tag{2}$$

A key hypothesis (confirmed by experiments) is that the spatial rate of change of volume flux (that is, the rate at which fluid is entrained into the jet) is proportional to the perimeter of the cross-section of the jet and the local mean velocity. This gives

$$\frac{dQ}{dz} = 2\alpha\pi ru \tag{3}$$

in which α is a dimensionless parameter to be determined by experimental data. Equations (1-3) can be used to give

$$\frac{Q}{r} = \frac{Q_0}{r_0} \tag{4}$$

$$\frac{Q}{Q_0} = 1 + \frac{2\alpha}{r_0}(z - z_0) \tag{5}$$

$$r = r_0 + 2\alpha(z - z_0) \tag{6}$$

$$\frac{u}{u_0} = \frac{1}{1 + 2\alpha(z - z_0)/r_0} \tag{7}$$

These results have been confirmed by experiments in jets with a wide variety of Reynolds numbers. Fischer *et al.* (1979, fig. 9.6) show the linear increase of the volume flux Q with z and provide the experimental value for the parameter α, namely $\alpha = 0.071$ (after allowing for the change in notation in Fischer's diagram).

An interesting feature of turbulent jets is that the results are independent of the nature of the fluid. All that is important is that the jet should be turbulent with Reynolds number greater than about 4000. This means that, in the case of a turbulent jet passing through an interface between two layers of fluid, there will be several important constant properties, namely the rate of increase of jet radius r with axial distance z, and the rate of increase with z of the volume flux Q. In other words, provided the jet is not deflected by the interface, its rate of spread will be as if the interface were not there.

4. Axisymmetric compartment model

The turbulent jet properties reviewed in the previous Section point the way to a simple compartment model which gives insight on how blending takes place. Suppose we have a turbulent jet directed upwards in the centre of a cylindrical tank of radius R and depth H as shown in figure 3. The notation is as introduced in Section 3. Imagine that the fluid contains a tracer whose concentration is denoted by $C(z, t)$. Initially this tracer will be all confined to one section of the tank, for example the top half, and it is desired to see how the tracer is dispersed by the action of the turbulent jet.

The two compartments in the model consist of the region in the jet and the region exterior to the jet (denoted by subscripts 1 and 2 respectively). The upwards flux of fluid in the jet is given by $Q(z)$, whilst the upwards flux in region 2 is $-Q(z)$. Assume that the tracer is perfectly mixed laterally at various heights in regions 1 and 2; thus the tracer concentrations $C_1(z, t)$ and $C_2(z, t)$ are functions of z and t and satisfy the equations

$$\pi r^2 \frac{\partial C_1}{\partial t} = -\frac{\partial}{\partial z}(QC_1) + C_2 \frac{dQ}{dz}$$

$$A(z) \frac{\partial C_2}{\partial t} = \frac{\partial}{\partial z}(QC_2) - C_2 \frac{dQ}{dz}$$

in which $A(z) = \pi[R^2 - r^2(z)]$ is the cross-sectional area of the region exterior to the jet. These equations can be re-written

$$\pi r^2 \frac{\partial C_1}{\partial t} = -Q \frac{\partial C_1}{\partial z} + (C_2 - C_1) \frac{dQ}{dz} \tag{8}$$

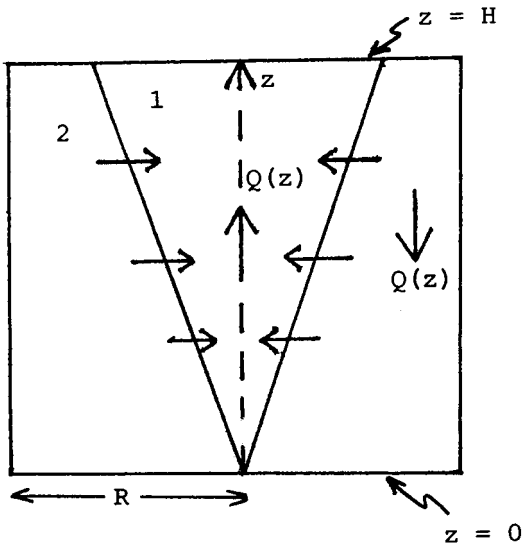

Figure 3: The compartment model for jet blending.

$$A(z)\frac{\partial C_2}{\partial t} = Q\frac{\partial C_2}{\partial z} \tag{9}$$

Suppose that fluid at the top of the jet is transported to the top of the exterior region, whilst material at the bottom of the exterior region is transported to the bottom of the jet. This gives the boundary conditions

$$C_1(0,t) = C_2(0,t), \quad C_1(H,t) = C_2(H,t) \tag{10}$$

As an initial condition, suppose that the tracer is confined to the top half of the tank, both in the jet and in the exterior region, that is

$$C_1(z,0) = C_2(z,0) = 0 \quad z < H/2 \tag{11}$$

$$C_1(z,0) = C_2(z,0) = 1 \quad z > H/2 \tag{12}$$

Equations (8-12) were solved by a simple numerical scheme that used explicit timestepping and upwind spatial differencing. That is, if the superscript n denotes time level and the subscript i denotes values at z_i, (8,9) were discretised using

$$C_{1_i}^{n+1} = C_{1_i}^n + \frac{\Delta t}{\pi r^2}\{-\frac{Q_i(C_{1_i}^n - C_{1_{i-1}}^n)}{\Delta z} + (C_2 - C_1)_i^n\frac{dQ}{dz}\}$$

$$C_{2_i}^{n+1} = C_{2_i}^n + \frac{\Delta t}{A(z_i)}\frac{Q_i(C_{2_{i+1}}^n - C_{2_i}^n)}{\Delta z}$$

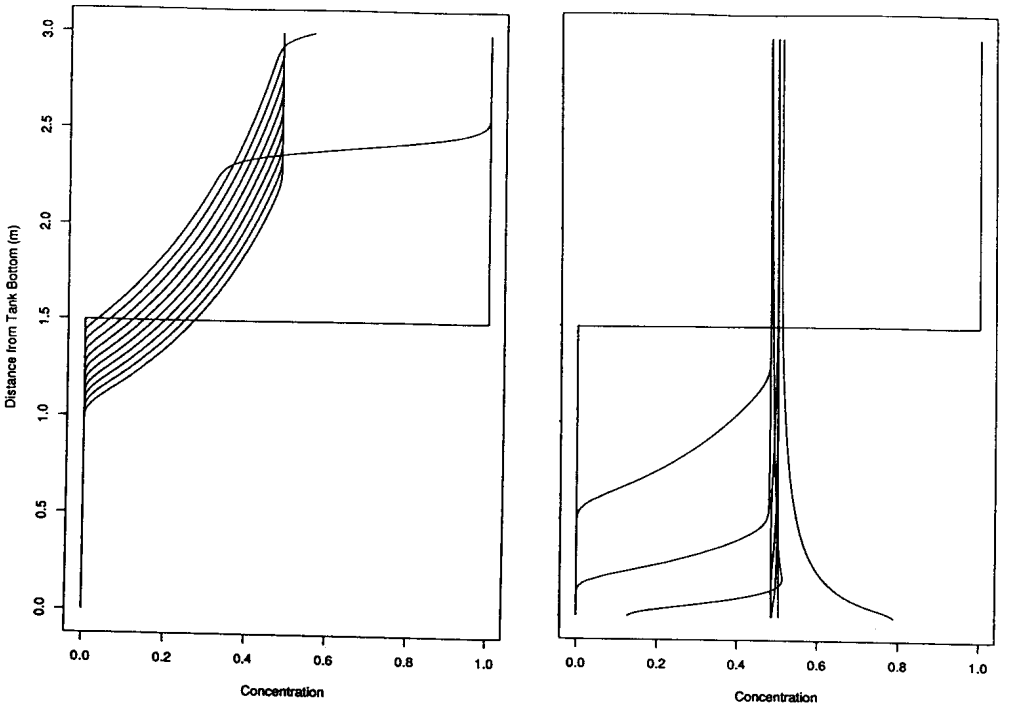

Figure 4: The concentration $C_1(z,t)$ of tracer interior to the jet for various values of t: LHS, time intervals of 0.75 sec; RHS, time intervals of 20 sec.

This numerical procedure converges provided the stability condition

$$max\{\frac{Q}{\pi r^2}, \frac{Q}{A(z)}\}\frac{\Delta t}{\Delta z} < 1 \tag{13}$$

is satisfied.

Numerical results for $C_1(z,t)$ and $C_2(z,t)$ are shown in figures 4 and 5 as a function of z at various values of time. In obtaining these results, we used the parameters R = 1.1 m, H = 3.0 m, Q_0 = 1000 lit/min, r_0 = 0.015 m. The results show how the tracer is mixed throughout the tank by the action of the turbulent jet.

A property of interest is the amount of time required for the tracer to be uniformly mixed. One way to examine this property is to plot $(C_{max} - C_{min})$ as a function of time, where

$$C_{max} = \overset{max}{0 < z < H} \quad \{C_1, C_2\}$$

$$C_{min} = \overset{min}{0 < z < H} \quad \{C_1, C_2\}$$

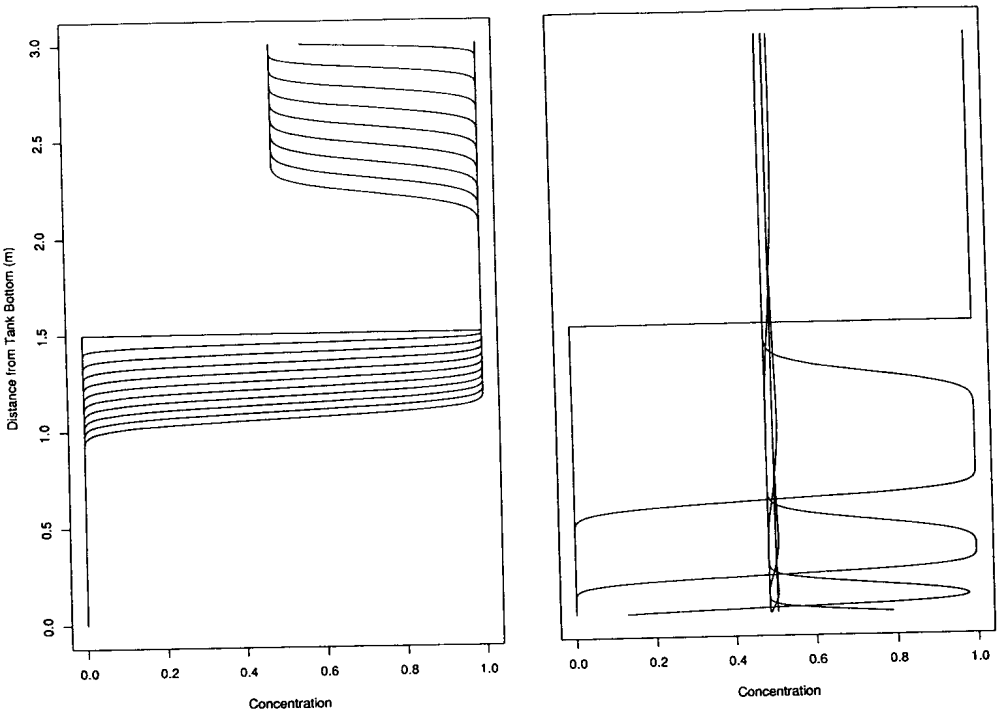

Figure 5: The concentration $C_2(z,t)$ of tracer exterior to the jet for various values of t: LHS, time intervals of 0.75 sec; RHS, time intervals of 20 sec.

Table 3. The parameter values used in figure 6.

result	H (m)	R (m)	Q (lit/min)	r_0 (m)
1	3.0	1.1	1000	0.015
2	3.0	1.1	1000	0.02
3	3.0	1.1	500	0.015
4	3.0	1.1	500	0.02
5	3.0	2.2	1000	0.015
6	3.0	2.2	1000	0.02
7	3.0	2.2	500	0.015
8	3.0	2.2	500	0.02

Results for $(C_{max}-C_{min})$ are shown in figure 6 as a function of time for the combination of parameter values shown in Table 3. We note that $(C_{max}-C_{min})$ is a demanding indicator of the extent of mixing. As a consequence, the results in figure 6 had to be computed with very fine meshes and small timesteps. The kinks shown in figure 6 occur when the surge of tracer moving downwards in region 2 reaches the bottom of the tank (see

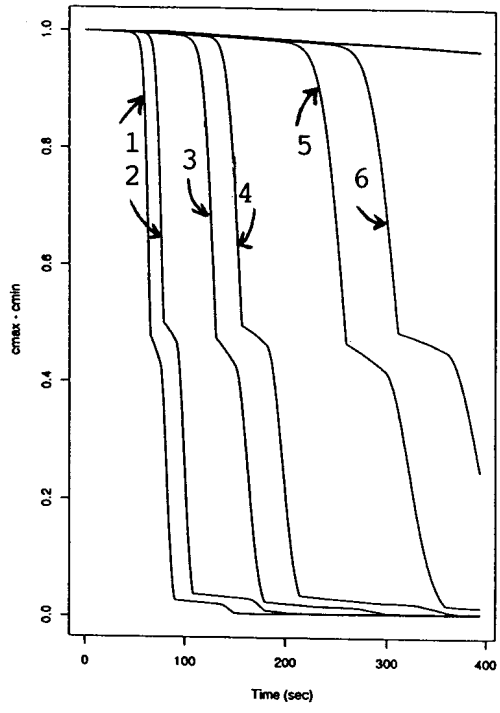

Figure 6: Illustrating $(C_{max} - C_{min})$ as a function of time for various combinations of parameter values.

figure 5, right hand side). This occurs on a much longer timescale than that required for the interchange of material between regions 1 and 2.

These results imply surprisingly quick mixing in small tanks with high volume flux pumps – for example, mixing should be more or less complete in these tanks within a couple of minutes. According to the results, tens of minutes would be required for mixing in large tanks with pumps of low volume flux. The nozzle radius has little effect on the mixing process.

The compartment model introduced in this Section probably gives a good model for transport and mixing processes in the jet itself, but assumes that mixing takes place instantaneously in the region exterior to the jet. *For this reason, the results underestimate the actual time required for the mixing process.* A better knowledge is required of mixing and flow effects external to the jet. This matter is addressed in the next Section.

5. CFD simulations

Another way to examine the blending of lubricants is by use of a commercial CFD

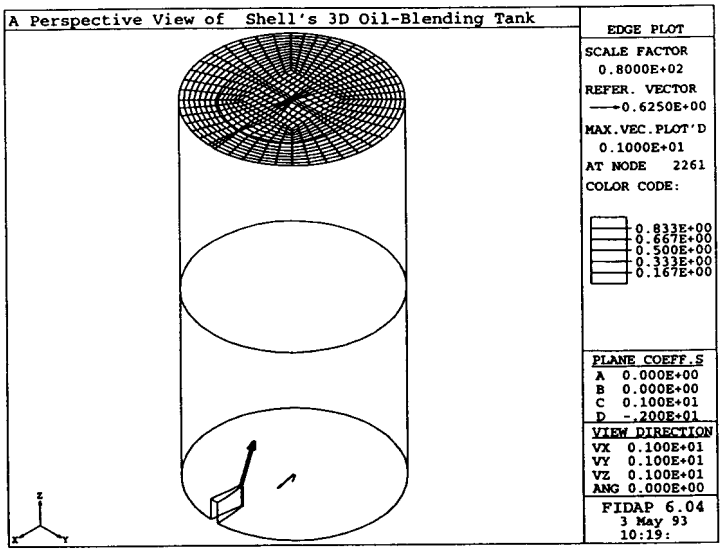

Figure 7: A perspective view of the oil-blending tank. The mesh in the circular cross-section is shown.

package. The CSIRO Supercomputing Facility and Australian Supercomputing Technology generously provided access to the finite element CFD code *FIDAP* on their supercomputers (CRAY Y-MP 4E/364 and Fujitsu VP2200 respectively).

Even with powerful computers and the best commercial software, it is a time-consuming task to set up a three-dimensional computational mesh and then predict the flow patterns caused by the submerged jet. Moreover, the code has limitations in how various layers of fluid can be handled. After some exploratory computations including a replication of the axi-symmetric model of section 4, computations were then made using the geometry shown in figure 7. In this geometry, the submerged nozzle is near the bottom and outside edge of the tank, and it points in a plane of symmetry through the centre of the tank. There is a drain in the bottom centre of the tank. The mesh in the cross-section is shown, and the computation was made with 20 layers in the vertical direction. Overall, the mesh involved 17068 elements and 15944 nodes, thus constituting a large CFD problem.

In this simulation, only one layer of oil was considered. For the oils we are dealing with in this blending process, it is realistic to assume that the fluid flow is incompressible, and therefore the incompressible Navier-Stokes equations are the governing equations for the fluid flow inside the tank. Since the flow is also turbulent with a high Reynolds number, a turbulence model is needed to close the governing equations. In this calculation, the widely used $k-\varepsilon$ model is adopted, and a wall-function approach

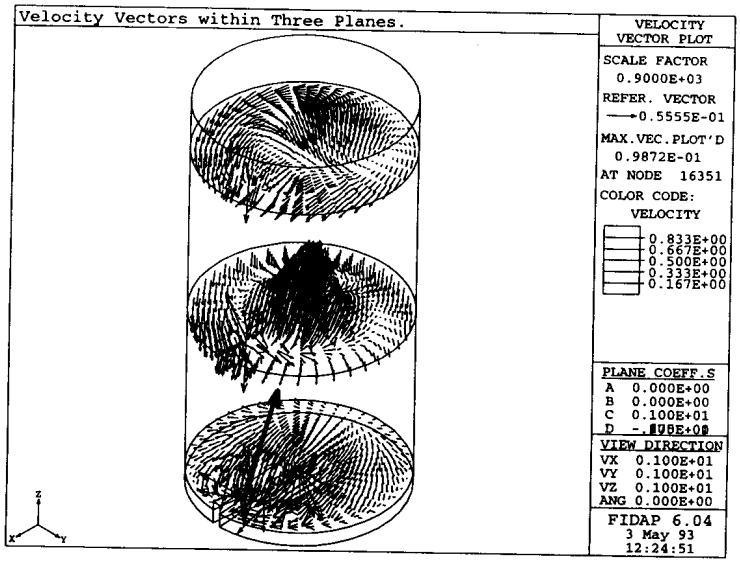

Figure 8: Velocity vectors at three horizontal slices in the tank.

is used near the solid walls.

For each of the node points of the 3D mesh, 3 velocity components (u, v, w), pressure p, and turbulence quantities k and ε need to be obtained by solving the governing equation system: the incompressible Navier-Stokes equations and the two extra transport equations for k and ε. To solve such a huge system, we have to rely on the segregated solution procedure, thus solving coupled equations in an uncoupled manner (see *FIDAP* Manual, vol 1). With this solution strategy, it takes about 22 hours of cpu time on the CRAY to obtain the solutions below.

In figure 7, the 3D tank is non-dimensionalized, the height being 2 and radius 0.5. The nozzle has a radius of 0.0064 and a nozzle speed of 1.0. The nozzle is positioned within the XZ symmetry plane and at an angle of less than 30^o from the Z-axis. The Reynolds number is set to 2.56×10^6, which corresponds to the nozzle Reynolds number of 3.3×10^4.

Figure 8 shows the velocity vectors at three different heights in the blending tank. In the centre slice, the coherent nature of the jet and the return flow around the outside of the jet are obvious. This figure gives a clear overall picture of the flow pattern inside the tank.

Figure 9 shows the velocity vectors in the plane of symmetry, and it confirms the coherent nature of the jet and the properties of the return flow. (The velocity jump detected in the region directly above the nozzle is caused by mesh over-concentration

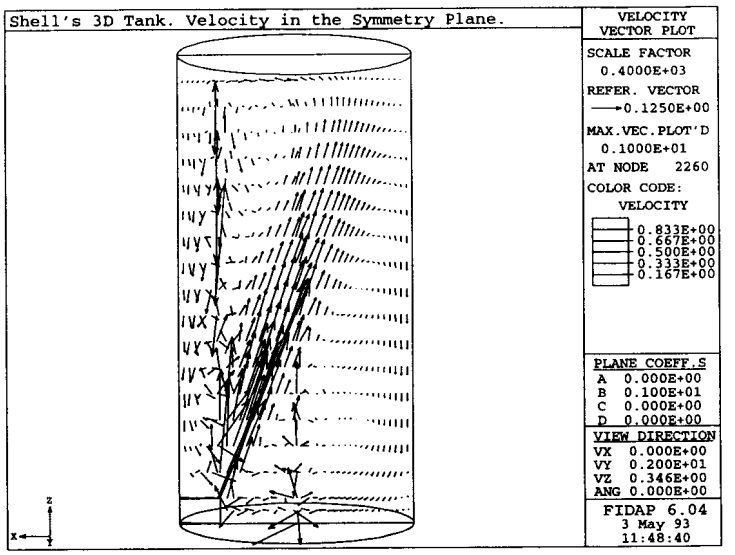

Figure 9: Velocity vectors in the plane of symmetry in the tank.

to represent the nozzle. Our tests show that this velocity surge does not influence the overall flow pattern prediction.) From this figure, we can clearly see that the fluid from the nozzle actually reaches the top region of the tank, which is in sharp contrast to the streamline contour shown in figure 10 from a corresponding 2D simulation. The 2D results show that the entrainment demand has caused a two cell structure to form in the flow. In the 3D case, the entrainment demand is met by flow all around the jet. From comparing these two figures, we can see that a 2D simulation in this case cannot truly reflect the three dimensional nature of the fluid flow pattern inside the tank.

The three dimensional nature of the flow can best be demonstrated in the streaklines shown in figure 11. The streaklines are the traces of massless particles released in flow regions of interest. From this figure, it can be seen that there are two large recirculation zones: one - the upper circulation zone of figure 11 - is formed primarily from the interaction of the jet with the top surface of the tank. The other is a secondary recirculation region which exists mainly due to entrainment. Since fluid flow within the secondary recirculation zone has a much smaller momentum level, fluid can easily form dead regions where mixing is slow. To increase the mixing, two aspects of the secondary recirculation zone need to be altered. One is to reduce the size of the recirculation zone, another is to increase the magnitude of fluid speed within this zone. Increasing the angle between the nozzle and the Z-axis is one way to accomplish the changes needed. However, further simulations are needed to determine the optimal angle so that best mixing can be obtained.

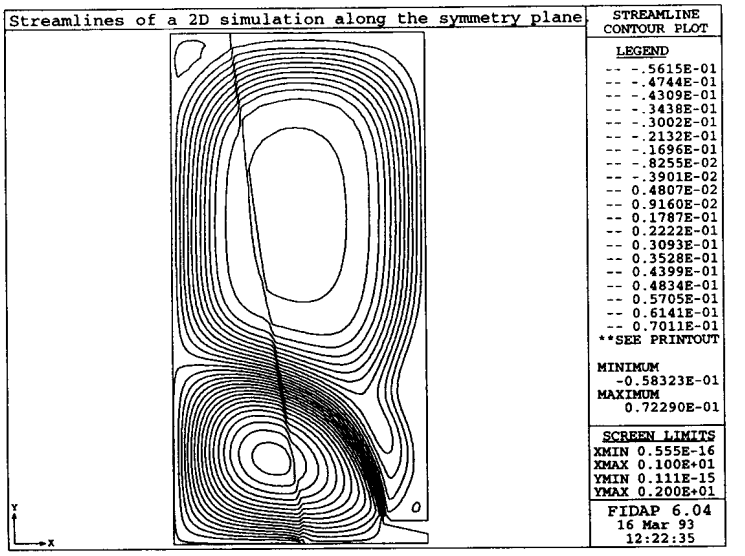

Figure 10: Streamlines for a two dimensional simulation.

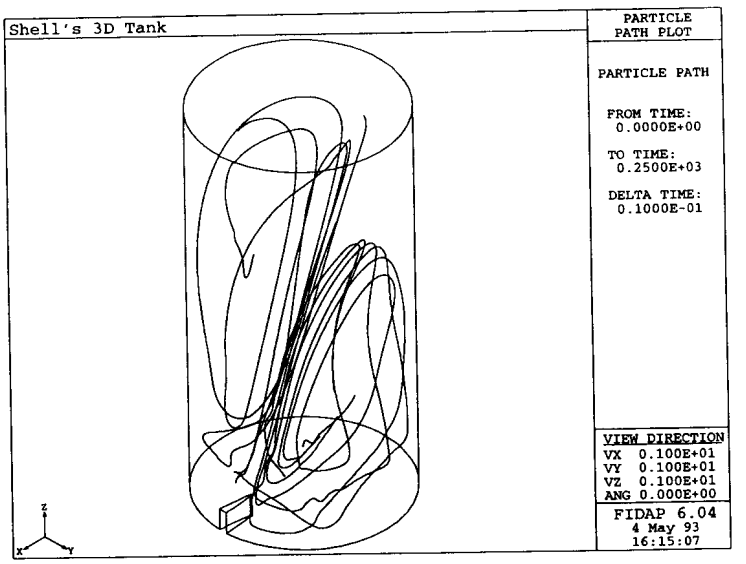

Figure 11: Streaklines for the three dimensional mixing problem.

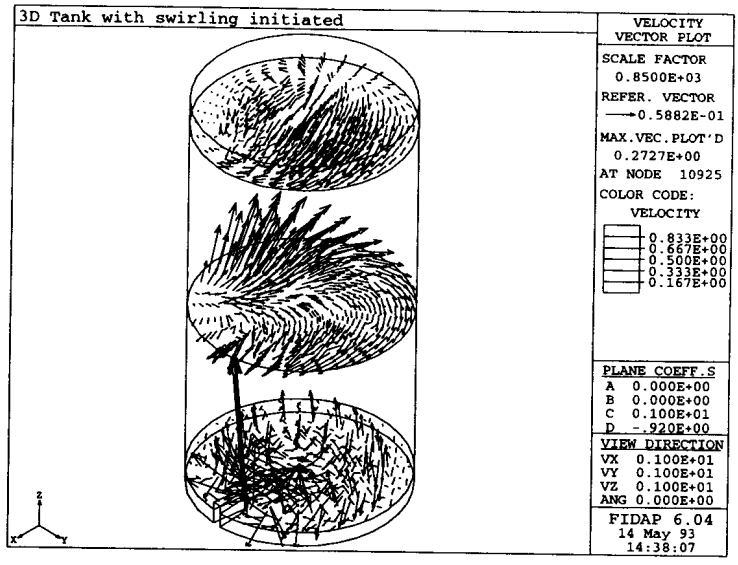

Figure 12: Velocity vectors at three slices in the tank for the helical flow.

CFD packages thus enable the effect of different nozzle placements to be investigated. An engineer could thus detect if there are dead zones where mixing is slow. For example, we can change the nozzle's angle with the Y-axis from 90^o to 120^o, so that the incoming fluid flow from the nozzle will form a helical flow pattern rather than being restricted within the symmetry XZ plane. Such a simulation would provide valuable information about whether helical swirling flow would increase mixing or not.

This simulation with swirl was carried out and the results are presented in figure 12. This shows the velocity vectors at the same three heights of the tank as presented in the earlier figure 8. In figure 12, there is a strong swirling flow pattern shown up at the centre slice; within the upper slice, this swirling flow is still evident except that flow stagnation can be detected on the left part of the upper slice. Figure 12 can best be complemented by the 3D particle traces presented as streaklines in figure 13. This shows that the region corresponding to figure 12's stagnation section has very little mixing around the point P_1. From the same figure, we find another secondary recirculation zone which is located around the point P_2. The existence of two regions of low mixing clearly demonstrates that by changing the nozzle's angle with the Y-axis from 90^o to 120^o, the mixing process actually becomes less efficient. This exercise shows that we are able to predict the flow patterns inside an oil-blending tank to see if a configuration of the tank and nozzle is efficient or not.

Once the flow field v has been computed, it is possible to track the evolution of concentration $C(x, t)$ of a tracer which has been injected into the flow. This would be

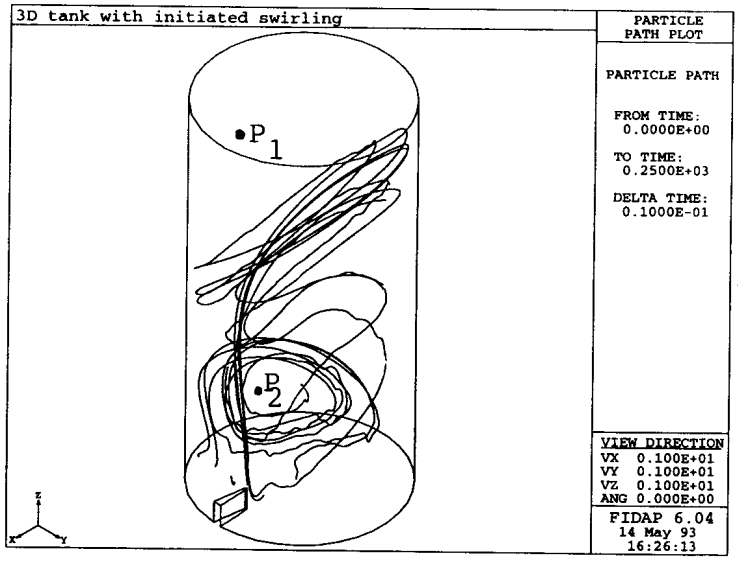

Figure 13: Streaklines for the helical flow simulation.

the extension of the compartment model explained in Section 4, and it would give a reliable indication of mixing times. As an indication, a tracer particle injected in the jet in figure 11 takes 10.3 seconds to reach the top of the tank and return to the bottom.

6. Sedimentation of contaminant particles

As mentioned in the Introduction, the oil mixtures to be blended contain contaminant particles whose number density is controlled by an International Standard. Specifically, in a 100 ml sample of oil, there can be no more than 130000 particles with diameter between 5 and 15 μm (1 μm = 10^{-6} m). These particles are metallic, silicates and wax.

The key issue to be addressed is how quickly will particles of this size sediment out of oil mixtures. First we show that the particles form an exceedingly low volume fraction of the oil. We then calculate the sedimentation rates of various particles, and finally we show that sedimentation is far more important than Brownian diffusion for these particles.

Consider the worst case scenario: 100 ml of oil containing 130000 particles of diameter 15 μm. The particles are assumed to be spherical. The volume of these particles is $130000 \times (4\pi/3)\ (7.5 \times 10^{-6})^3 = 2.297 \times 10^{-10}$ m^3. The ratio between the volume of the oil and particles is 435000:1 – an exceedingly low volume fraction of particles. Moreover, a simple calculation shows that the particles are separated by at

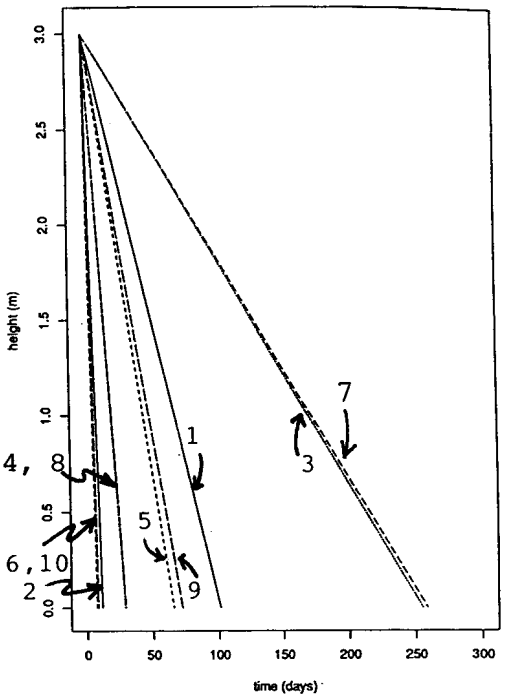

Figure 14: Sedimentation of particles of various sizes.

least 60 particle radii. Under these circumstances, each particle will fall slowly through the oil completely independent of the other particles.

The speed of sedimentation is given by Stokes Law:

$$\frac{4\pi g}{3} r_0^3 (\rho_{particle} - \rho_{oil}) = 6\pi\mu U_{Stokes} r_0$$

where r_0 is the particle radius and μ is the fluid viscosity. This yields

$$U_{Stokes} = \frac{2r_{0g}^2}{9\mu}(\rho_{particle} - \rho_{oil}) \tag{14}$$

With this result, we can plot the rate of sedimentation of various particles through a typical oil mixing tank 3 m in height. The results displayed in figure 14 shows that it takes days, sometimes many days, for the particles to sink through the mixing tank.

result	material	radius μ	days to fall through 3 m
1	rust	2.5	101
2	rust	7.5	11
3	aluminium	2.5	255
4	aluminium	7.5	29
5	steel	2.5	65
6	steel	7.5	7
7	silicates	2.5	259
8	silicates	7.5	29
9	cast iron	2.5	72
10	cast iron	7.5	8

It is of interest to compare these sedimentation times with the time for fluid motions to decay away. Batchelor (1970, 5.4.5) shows that the final decay of turbulent energy is exponential with e-folding time $\tau = 1/(2\nu\lambda^2)$ where λ is the wave number of the largest eddies. Inserting $\lambda = 2\pi/H$ and the values $\nu = 5 \times 10^{-5}$ m^2/s and H=3m gives τ = 38 minutes. That is, it takes *much* longer for most particles to sediment than it does for the fluid to reach a steady state after mixing.

We also consider the effect of Brownian motion on the steady settling of particles under Stokes Law. Brownian motion causes a diffusion-like effect with diffusion coefficient (Levin, 1978, equation 16.49)

$$D = \frac{kT}{6\pi r_0 \mu} \tag{15}$$

in which k is Boltzmann's constant. The concentration of particles with height z is described by the equation

$$D\frac{d^2C}{dz^2} + U_{Stokes}\frac{dC}{dz} = 0 \tag{16}$$

under the boundary conditions

$$C(\infty) = C_0, \qquad C(0) = C_{max}$$

The concentration $C(z)$ is

$$C = C_0 + (C_{max} - C_0)\, e^{-zU_{Stokes}/D} \tag{17}$$

This concentration is equal to C_0 throughout most of the range of z, and adjusts rapidly to C_{max} in a boundary layer of thickness $O(D/U_{stokes})$ where

$$D/U_{Stokes} = \frac{3kT}{4\pi r_0^3 g(\rho_{particle} - \rho_{oil})} \tag{18}$$

[This result can be interpreted by recognizing that the boundary layer is a balance between the energy kT of random oscillations and the work done by buoyancy in moving the particle through the height of the boundary layer.] Insertion of typical values for the constants in (18) shows that the boundary layer is miniscule, namely about 5.98×10^{-12} m in height. That is the particles at the large end of the allowable range are not affected for practical purposes by Brownian motion. Particles of one tenth the maximum size will similarly be unaffected.

7. Conclusions

As a result of this investigation:

- We acquired a good understanding of the overall mixing process.
- We used a series of conceptual models with increasing degrees of realism to obtain estimates for mixing times.
- We developed a good framework for CFD simulations of oil blending; particularly through an understanding of the necessity of 3D models, and derivation of simulation results for mixing with and excluding swirling flow. These results show that engineering design issues can be addressed using CFD simulations.
- We acquired a good understanding of the sedimentation of contaminant particles in oil, and knowledge of sedimentation times for various species of particles.

Acknowledgements

This problem was co-moderated by Noel Barton, Steve Spencer and Zili Zhu. We are grateful to Colin Macpherson of Shell for his involvement, and to the large team who contributed to work on the problem, particularly John Hunter, Bernhard Neumann, and Sean McElwain and his students.

References

G.K. Batchelor, *The Theory of Homogeneous Turbulence* (Cambridge University Press, 1970).

H.B. Fischer, J. Imberger, E.J. List, R.C.Y. Koh & N.H. Brooks, *Mixing in Inland and Coastal Waters* (Academic Press, 1979).

I.R. Levin, *Physical Chemistry* (McGraw Hill, NY, 1978).